dc to 40 GHz Coaxial-to-Microstrip Transition for 100-μm-Thick GaAs Substrates

JOSEPH CHENKIN, MEMBER, IEEE

Abstract—**The design, design approach, and test results are presented for a simple coaxial-to-microstrip transition. The approach provides improved performance over the basic coaxial-to-microstrip transition by causing a TEM-to-quasi-TEM transformation through a tapering of the coaxial line for 432 ± 51 μm ($\leqslant 6$ percent of λ_0 at 40 GHz) prior to impinging a portion of the resultant quasi-TEM field directly across the microstrip's dielectric at the coaxial–microstrip interface. Tests show that the return loss for the transition into a 50 Ω microstrip line on a 100-μm-thick GaAs substrate is better than 16.9 dB per transition from 200 MHz to 40 GHz. A cover having a height of 1.9 mm and a width of 2.6 mm had little or no influence on test results.**

I. Introduction

The requirement to test single devices and microstrip circuits made on 100-μm-thick GaAs substrates imposed the need to design, fabricate, and test a transition. Because the existing test equipment from 45 MHz to 26.5 GHz has coaxial connectors, and waveguide-to-coaxial transitions were available for the *Ka*-band, a coaxial-to-microstrip transition was chosen.[1]

The basic method for making a coaxial-to-microstrip transition is to solder the outer conductor of the coaxial cable to the microstrip's ground plane and the inner conductor to the microstrip. A method for improving this configuration was published by England [1] in 1976, in which he removed a portion of the microstrip's ground plane at the coaxial–microstrip interface, thereby reducing the discontinuity capacitance. A U.S. patent was awarded to Eisenhart [2] in 1981 for a second method of improving the basic end-launch design; in this modification, the center conductor is tapered and shifted off center toward the wall of the outer conductor to improve the field match at the coaxial-to-microstrip transition. The basic launcher has been used in *W*-band as part of a waveguide-to-coaxial-to-microstrip transition for 50-μm-thick substrates by Neidert [3], yielding a *VSWR* of better than 1.8:1 (return loss 10.9 dB) per transition.

The above transitions do not provide for a physical alignment of the microstrip and coaxial ground planes. These designs work well for thicker substrates where a slight ground plane misalignment may improve performance by introducing a step discontinuity. In Fig. 1 a typical step discontinuity is shown. The design presented in this paper leads to improved performance through two mechanisms:

1) A transformation of the TEM mode field that has propagated within the standard concentric cylindrical coaxial cable into a quasi-TEM field configuration via the mode transduction imposed by a nonstandard section of coaxial line. Within the nonstandard section the distance between conductors decreases linearly while maintaining an outer to inner conductor diameter ratio constant and corresponding to a characteristic impedance of 50 Ω.

Manuscript received February 29, 1988, revised January 26, 1989

The author is with Martin Marietta Laboratories/Gamma Monolithics (a partnership of Martin Marietta Corporation and Alpha Industries, Inc.), 1450 South Rolling Road, Baltimore, MD 21227.

IEEE Log Number 8927790

[1]Test equipment with coaxial connectors is now available for 0.04–40 GHz.

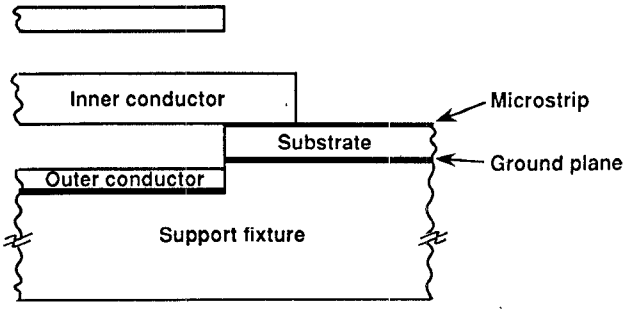

Fig. 1 A typical step discontinuity at a coaxial-to-microstrip interface.

TABLE I

	Eisenhart's [2]	New Transition
Length, μm	25400	432 ± 51
Length, $\lambda_{0.18\,GHz}$	1.525	0.026

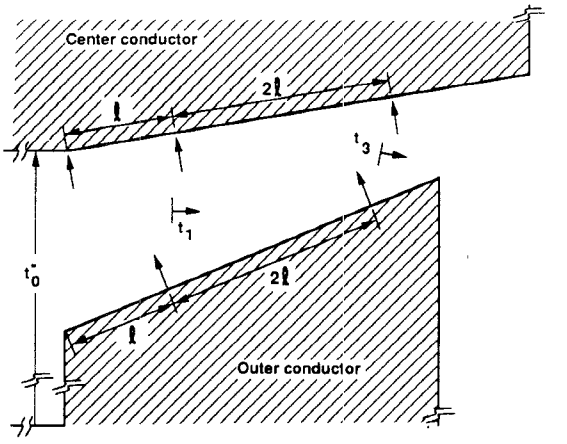

Fig. 2. A cutaway scaled view of the design.

2) A portion of the resultant quasi-TEM field is then launched directly across the microstrip's dielectric at the coaxial–microstrip interface.

Table I compares the length of the transition region for the best of the previous transitions and the new transition.

II. Design Approach

Fig. 2 is a cutaway scaled view of the design showing a short section of standard coaxial cable followed by the tapered region. Even though the taper is linear, the angles of diversion from the longitudinal axis of the inner and the outer conductor are different. This sets up the conditions for a transfer of energy from the transverse $\boldsymbol{E}$ and $\boldsymbol{H}$ fields into a longitudinal component as follows:

a) Within the standard coaxial section, the inner and outer conductors are parallel; the longitudinal components of $\boldsymbol{E}$ and $\boldsymbol{H}$ are 0.

b) Within the tapered coaxial section, the inner and outer conductors are not parallel, causing a bending of the radial $\boldsymbol{E}$ field to maintain the field perpendicular at the conductor–dielectric boundary. This causes energy to be trans-

ferred from the TEM field into a longitudinal component that is not tangential to either conductor [4].

A less obvious phenomenon contributing to the field transformation can be seen by looking in more detail at Fig. 2. The field at time t_0 enters the tapered region, where as the wave propagates it moves further longitudinally along the center conductor–dielectric interface than along the dielectric–outer conductor interface for any finite time increment. Given that the angle from horizontal is 10.01° for the inner conductor and 22.38° for the outer conductor, it can be calculated that the field propagates l ($\cos 10.01° - \cos 22.38°$) further longitudinally at the inner conductor–dielectric interface by the end of time interval t_1. A line drawn to trisect the dielectric–conductor interfaces at lengths l and $3l$ is tangential to the field front at times t_1 and t_3, respectively. Given that length l equals 127 μm, the angles from a line perpendicular to the conductors to the tangential lines can be determined. Solving the trigonometric problem yields for the outer conductor at t_1 an angle of 24.81° and at t_3, 32.05°. Similar calculations for the inner conductor yield at t_1 an angle of 12.43° and at t_3, 19.68°. During the calculations to determine the above angles, the angle contribution due to the difference in horizontal propagation was obtained, equaling 2.43° at t_1 and 9.67° at t_3.

Thus, the transformation of TEM energy into radial and longitudinal components is proportional to the cosine and sine of the angles between the lines perpendicular to the conductors and the lines drawn to trisect the dielectric–conductor interfaces at lengths l and $3l$. From this it can be inferred that a significant portion of the original TEM wave has gone into a longitudinal component.

A commercial connector/launcher[2] was chosen as the base of the transition. The launcher was then modified for the improved field match at the coaxial–microstrip interface. Fig. 3 shows a standard connector/launcher and an enlargement of the area modified, along with a section of microstrip. The launcher was modified in two places: 1) the center conductor of the glass bead on the microstrip side; and 2) the housing within which the glass bead is inserted, so that the outer conductor for the modified glass bead's center conductor would have the dimensions necessary to maintain the correct ratio for a 50 Ω line.

Two launchers were built into a test fixture for input (port 1) and output (port 2) connectors. The ports were interconnected with a 50 Ω microstrip through-line made on a GaAs substrate 0.1 mm thick, 2.54 mm wide, and 25.4 mm long.

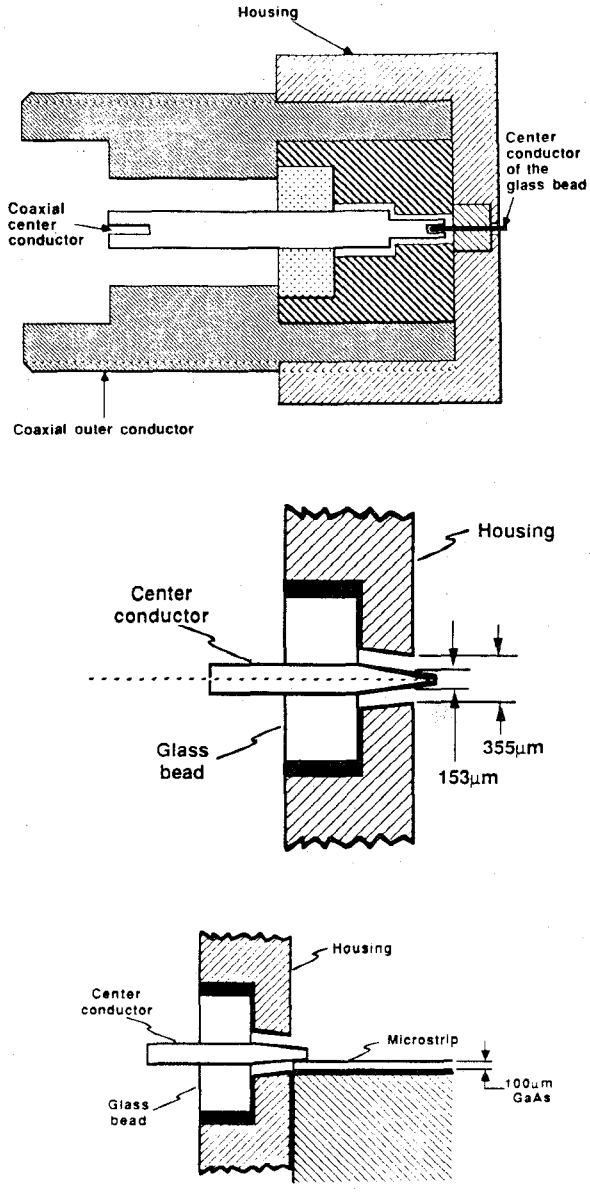

Fig. 3. A standard connector/launcher and an enlargement of the modified area.

III. Test Data

The test fixture's return loss for port 1's coaxial-to-microstrip transition was separated from those of port 2 using time-domain signal processing.[3] A time window (time gate) was placed around the required information, blocking out the reflection from the second port.

The return losses were better than 16.9 and 17.9 dB per transition from 200 MHz to 40 GHz for ports 1 and 2, respectively. The insertion loss $|S_{21}|$ for the two transition/through-line combination was less than 3.5 dB at 40 GHz; time-domain signal processing was not used during the S_{21} measurements.

Fig. 4(a) shows the return losses of both transitions in the time domain as measured through port 1. After imposing a time window across port 1's measured reflection, the data shown in Fig. 4(b) were taken. Fig. 4(c) shows the same data after being transformed back into the frequency domain. In Fig. 4(d) $|S_{21}|$ versus frequency is presented. Fig. 5(a)–(c) shows data similar to those of Fig. 4(a)–(c) for the test fixture as measured through port 2.

Fig. 5(d) shows group delay for S_{21}.

The data shown are for an enclosed substrate, and were essentially the same with or without a cover for two reasons:

1) The cover, with cross-sectional dimensions of 2.6 mm wide by 1.90 mm high (Fig. 6), was large enough that it did not significantly change the microstrip's characteristic impedance and thereby cause a change in performance.
2) The radiative loss did not appreciably change under covered or uncovered conditions, possibly because the coaxial-to-microstrip transition launches a quasi-TEM mode into the quasi-TEM mode medium.

[2]K Connector is a trademark of Wiltron.
[3]Test data courtesy of Wiltron (0.04–40 GHz test set with coaxial connectors).

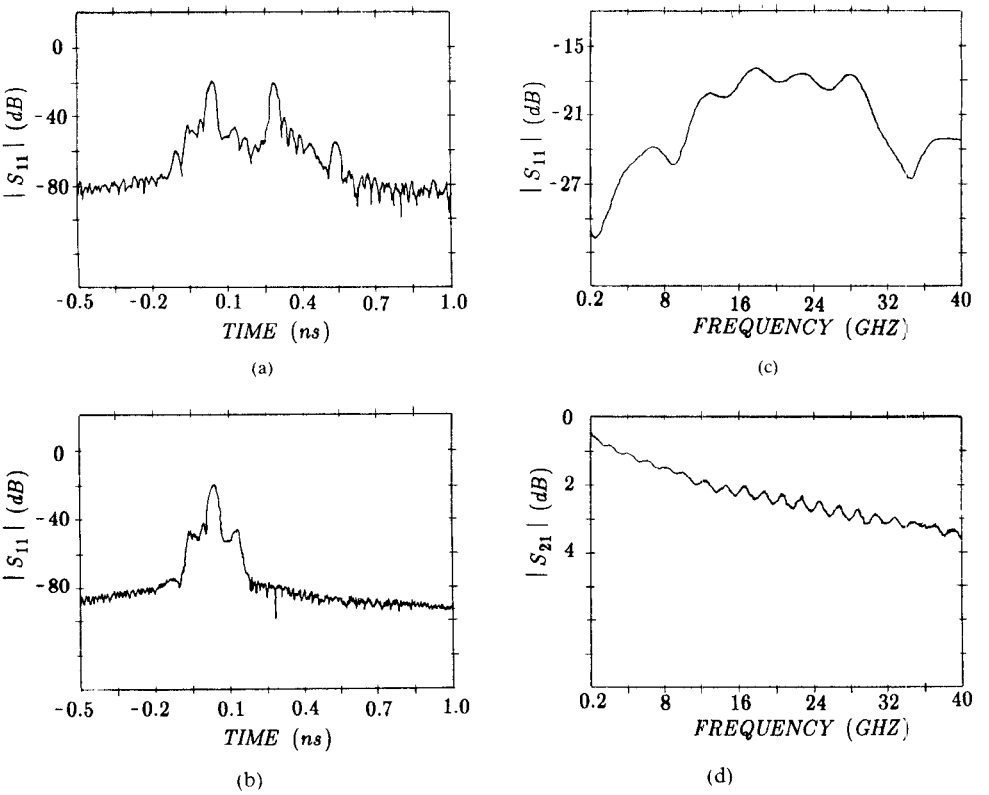

Fig. 4. (a) $|S_{11}|$ versus time for two back-to-back transitions separated by a 25.4-mm-long 50 Ω microstrip on a 100-μm-thick GaAs substrate. (b) $|S_{11}|$ versus time after a time gate has been applied. (c) $|S_{11}|$ versus frequency with the same time gate as applied in (b) (d) $|S_{21}|$ versus frequency without a time gate applied.

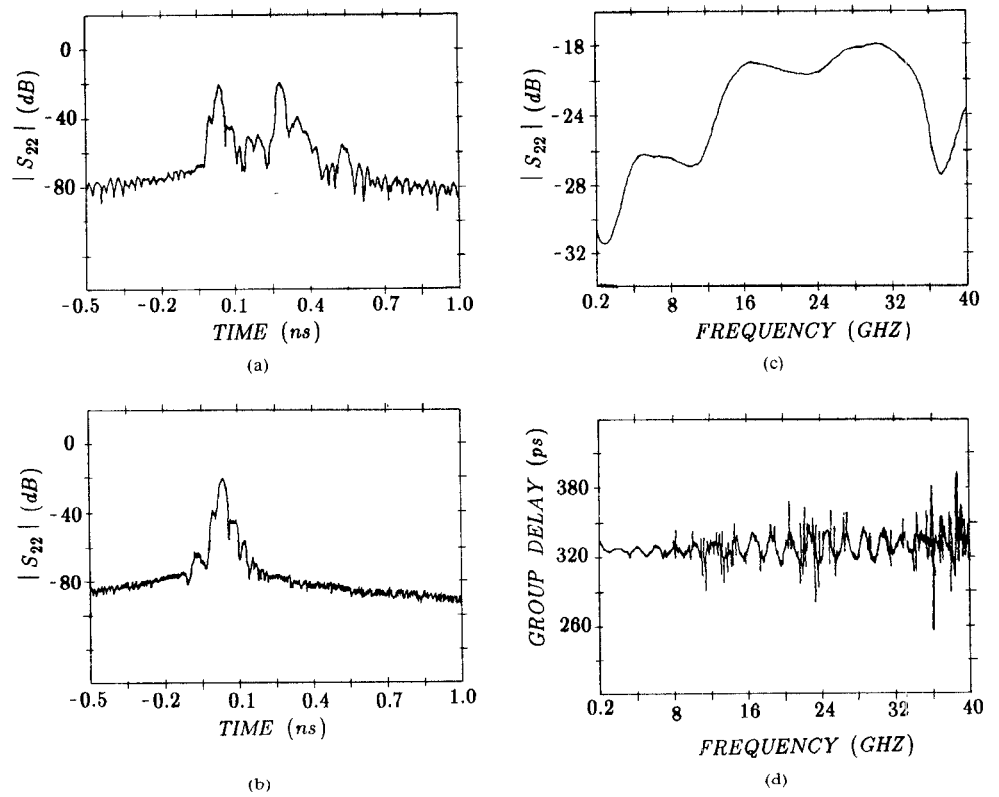

Fig. 5 (a) $|S_{22}|$ versus time for the same test structure shown in Fig. 4. (b) $|S_{22}|$ versus time after a time gate has been applied (c) $|S_{22}|$ versus frequency with the same time gate as applied in (b). (d) Group delay versus frequency without a time gate applied.

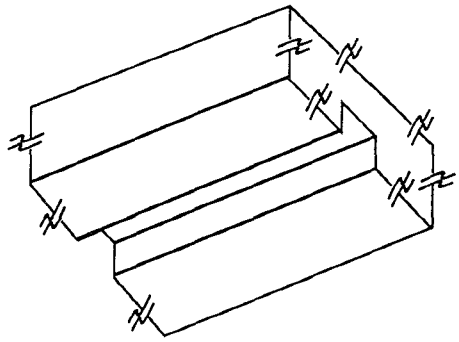

(a)

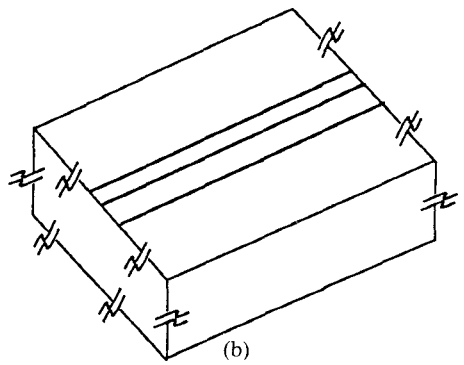

(b)

Fig 6 (a) The cover in relation to (b) the substrate attached to the substrate carrier

IV. Conclusions

A design approach that is simple in concept, that does not require an expert level of understanding to implement, and that presents a workable solution to the fundamental packaging problem of injecting and extracting energy from a hybrid or monolithic circuit has been presented.

References

[1] E. H. England, "A coaxial to microstrip transition," *IEEE Trans. Microwave Theory Tech*, vol MTT-24, pp. 47–48, Jan 1976

[2] R L Eisenhart, "Electrical coupler," U.S. Patent: 4 280 112, July 21, 1981.

[3] R. E Neidert, "Waveguide-to-coax-to-microstrip transition for millimeter-wave monolithic circuits," *Microwave J*, vol. 26, pp. 93–101, June 6, 1983

[4] N. Marcuvitz, Editor, *Waveguide Handbook*. New York. Dover, 1965, pp. 47–54.

A Note on the Mixed Potential Representation of Electric Fields in Layered Media

M. J. CLOUD, MEMBER, IEEE, AND D. P. NYQUIST, MEMBER, IEEE

***Abstract*—A mixed potential formulation is given for electric fields in layered environments. Contributions to the field from charges are identified explicitly through a scalar Green's function for layered media. The outcome is a computationally expedient Sommerfeld integral representation.**

Manuscript received May 27, 1988; revised January 23, 1989. This work was supported in part by the National Science Foundation under Grant ECS-86-11958 and by the Office of Naval Research under Contract N00014-86-K-0609.

M. J. Cloud is with Lawrence Technological University, Southfield, MI 48075.

D. P. Nyquist is with the Department of Electrical Engineering, Michigan State University, East Lansing, MI 48824-1226

IEEE Log Number 8927788.

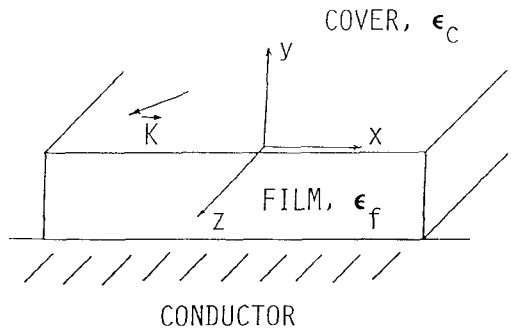

Fig. 1 Configuration of layered media.

I. Introduction

The study of electric fields due to surface currents in millimeter-wave integrated circuits [1], [2] brings to light certain facts about the alternative representation of Hertz potentials. Despite their apparent simplicity, these observations have not appeared previously in this form. The points discussed in this paper bear directly upon the divergent spectral integrations which have been offered on several occasions [3], [4] in the recent literature; it is hoped that ultimately they will find application in avoiding comparatively awkward formulations.

II. Hertz Potential Green's Dyad Formulation

Consider the configuration of layered dielectric media over a conducting half-space as shown in Fig. 1. The electric field $\vec{E}(\vec{r})$ in the cover, maintained by surface currents embedded in that same layer, decomposes linearly into two parts as $\vec{E}(\vec{r}) = \vec{E}^p(\vec{r}) + \vec{E}^r(\vec{r})$. The fields of the right member may be termed the primary and reflected components. A Hertz potential representation of $\vec{E}$ based upon this decomposition is given by Bagby and Nyquist [1], [2] as follows:

$$\vec{E}(\vec{r}) = \left(k_c^2 + \nabla\nabla\cdot\right)\int_S \vec{\vec{G}}(\vec{r},\vec{r}')\cdot\left[\vec{K}(\vec{r}')/j\omega\epsilon\right] dS' \quad (1)$$

where $\vec{K}(r)$ describes source currents on surface S, and $\vec{\vec{G}} = \vec{\vec{I}}\, G^p + \vec{\vec{G}}^r$ is the decomposition of the Hertz potential Green's dyad into primary and reflected components. The dyad scalar components are given as double spectral (Sommerfeld-type) integrals:

$$G^p(\vec{r},\vec{r}') = \iint_{-\infty}^{\infty} \frac{\exp\left[j\vec{\lambda}\cdot(\vec{r}-\vec{r}')\right]\exp\left[-p_c|y-y'|\right]}{2(2\pi)^2 p_c} d^2\lambda \quad (2)$$

$$\begin{pmatrix} G_t^r(\vec{r},\vec{r}') \\ G_n^r(\vec{r},\vec{r}') \\ G_c^r(\vec{r},\vec{r}') \end{pmatrix} = \iint_{-\infty}^{\infty} \begin{pmatrix} R_t(\lambda) \\ R_n(\lambda) \\ C(\lambda) \end{pmatrix} \frac{\exp\left[j\vec{\lambda}\cdot(\vec{r}-\vec{r}')\right]\exp\left[-p_c|y-y'|\right]}{2(2\pi)^2 p_c} d^2\lambda \quad (3)$$

where $\vec{\vec{G}}^r = \hat{x}G_t^r\hat{x} + \hat{y}[(\partial G_c^r/\partial x)\hat{x} + G_n^r\hat{y} + (\partial G_c^r/\partial z)\hat{z}] + \hat{z}G_t^r\hat{z}$. The R_t, R_n, and C are reflection and coupling coefficients detailed in [1] and [2]. Note that $p_c = [\lambda^2 - k_c^2]^{1/2}$ is a wavenum-

0018-9480/89/0700-1150$01.00 ©1989 IEEE